*Proc. Natl. Acad. Sci. USA*
Vol. 87, pp. 8820–8824, November 1990
Cell Biology

# Microtubule dynamics in living dividing plant cells: Confocal imaging of microinjected fluorescent brain tubulin

DAHONG ZHANG, PATRICIA WADSWORTH, AND PETER K. HEPLER

Departments of Botany and Zoology and Program in Molecular and Cellular Biology, University of Massachusetts, Amherst, MA 01003

*Communicated by Lynn Margulis, June 22, 1990 (received for review May 11, 1990)*

ABSTRACT **Carboxyfluorescein-labeled brain tubulin has been microinjected into stamen hair cells of *Tradescantia*, and its distribution during mitosis and cytokinesis was examined using confocal laser scanning fluorescence microscopy. The results show that brain tubulin incorporates into plant microtubules and is utilized throughout mitosis and cytokinesis. Microtubule structures that incorporate brain tubulin include the preprophase band, the perinuclear sheath at late prophase, the kinetochore fibers during prometaphase, metaphase, and anaphase, the interzone spindle during anaphase, and finally the phragmoplast during late anaphase and telophase. All of these microtubule-containing structures and, notably, their transitions from one to another have been observed in single live cells progressing through mitosis and cytokinesis.**

The structure of the mitotic and cytokinetic apparatuses in plant cells has received considerable attention from electron microscopic and immunofluorescence studies (1–6), in which the form and distribution of microtubules (MTs) in the principal stages have been revealed. Unfortunately, because of the necessity of fixing cells either for electron microscopy or for immunocytochemistry, it has not been possible to examine the dynamics of MT formation, breakdown, and reformation that accompanies the transitions between the mitotic stages. Important dynamic information, of course, has been obtained from polarized light microscopic studies (7), especially from observations of mitosis in cultured liquid endosperm cells (8, 9). Despite the power and elegance of this method, it has certain serious limitations when applied to plant cells that typically have a cellulose wall. Because of the strong birefringence arising from the cellulose, it is extremely difficult to resolve the much weaker birefringence of the underlying spindle apparatus.

To observe MT dynamics in living plant material, we have applied the technique of fluorescent analogue cytochemistry (10–13) to dividing stamen hair cells of *Tradescantia*. We have microinjected carboxyfluorescein-labeled brain tubulin into dividing cells and examined the fluorescence signal using a confocal laser scanning microscope (CLSM) (14). With this method we have observed complete mitotic sequences in which the tubulin fluorescence has been recorded at frequent time points in a single cell thus providing direct information on the dynamics of MTs from prophase, through spindle assembly, chromosome motion, and cell plate formation.

## MATERIALS AND METHODS

**Cell Culture.** Stamen hairs were obtained from immature buds of *Tradescantia virginiana*, immobilized in a thin film of low-temperature-gelling agarose (1%), and cultured in a medium containing 5 mM KCl, 0.1 mM $CaCl_2$, and 5 mM Hepes (pH 7.0) (15).

**Preparation of Fluorescently Labeled Brain Tubulin.** Purified tubulin, isolated from pig brain by molecular sieve chromatography (16), was labeled with 5(6)-carboxyfluorescein succinimidyl ester (NHS-Fl) (Molecular Probes) following the method of Vigers *et al.* (17) with the following modifications. Pure tubulin was polymerized in a buffer containing 4 M glycerol, 10 mM $MgSO_4$, 0.1 M Pipes (pH 6.9), and 2 mM EGTA. NHS-Fl was added at a dye-to-tubulin molar ratio of 40:1 and incubated for 10 min at 37°C. The MTs were then sedimented through a sucrose cushion and subjected to two additional cycles of temperature-dependent assembly and disassembly in glutamate buffer (1 M sodium glutamate/2 mM EGTA/1 mM $MgSO_4$, pH 6.9). The final pellet was resuspended in injection buffer (20 mM sodium glutamate/0.5 mM $MgSO_4$/1 mM EGTA), incubated at 4°C to disassemble the MTs, and centrifuged. The resulting supernatant was frozen in liquid nitrogen and stored at −70°C. The dye-to-protein ratio was 0.5, as determined using an extinction coefficient of 48,000 at 495 nm for NHS-Fl.

**Microinjection of Tubulin into Stamen Hair Cells.** Micropipettes, constructed from borosilicate glass capillaries (World Precision Instruments, New Haven, CT) on a vertical pipette puller (model 700, David Kopf Instruments, Tujunga, CA), were loaded with centrifuged tubulin (2 min at 13,000 rpm in a Beckman Microfuge) using a thinly drawn plastic syringe. The pipette was mounted in a Zeiss microneedle holder, which was connected to a 2.0-ml micrometer syringe (Gilmont Instruments, Barrington, IL) by a water-filled polyethylene tubing (internal diameter, 0.38 mm). Hydraulic pressure was used to drive the protein into the cell. A micromanipulator (model 103R, Narishige Scientific Instrument Laboratory, Tokyo) was used for precise micropipette maneuvering.

Microinjections were performed on an inverted microscope (Zeiss, model IM-35) equipped with Nomarski optics. Tip cells in prophase were selected for microinjection. Before impalement, a slight positive holding pressure was applied to the micropipette preventing back flow of cytoplasm into the pipette. After a shallow penetration, protein solution was hydraulically pushed into the cell, and a volume was introduced that caused the transverse cross wall at the base of the cell to bow outward. To roughly calibrate this volume, we injected silicone oil until it caused a similar bowing of the cross wall, measured the diameter of the droplet, and determined that about 1% of the total cell volume was injected. Since the tubulin in the injection pipette is 3 mg/ml, we calculate that the final concentration of injected tubulin in the cell is ≈0.3 μM. Once the protein has been introduced, it is important to remove the micropipette slowly (5–15 min) from the cell, allowing the formation of a callose plug that heals the wound site.

**CLSM.** Cells injected with fluorescently labeled protein were imaged on a CLSM (MRC-500, Bio-Rad Microscience Divisions). The full power (10 mW) argon ion laser excitation

The publication costs of this article were defrayed in part by page charge payment. This article must therefore be hereby marked "*advertisement*" in accordance with 18 U.S.C. §1734 solely to indicate this fact.

Abbreviations: CLSM, confocal laser scanning microscope; MT, microtubule.

light (488 nm) was reduced in its intensity by a (1% transmission) neutral density filter (ND = 2) to minimize bleaching of the fluorophores and damage to the cell. A high numerical aperture (1.4 NA, 60×) oil-immersion lens was used to maximize the collection of the emitted fluorescent light. For studies involving sequences throughout mitosis, a thin (2 μm) optical section from the midplane of the cell was scanned ≈20 times (Kalman averaging) to form one image. Between taking fluorescent images, mitotic progression was closely followed using bright-field optics. Images obtained after background subtraction and contrast enhancement with the MRC-500 processor were photographed directly from the video screen using Kodak T-Max 400 film.

## RESULTS

Microinjected carboxyfluorescein-labeled brain tubulin incorporated into the preprophase band, the perinuclear clear zone, the mitotic apparatus, and the phragmoplast. The pattern of fluorescence was remarkably similar to that of MTs in other dividing plant cells, as determined by a variety of techniques, including especially indirect immunofluorescence with anti-tubulin antibodies (5, 6, 18–21) and electron microscopy (1, 22–24). We conclude, therefore, that the brain tubulin copolymerizes with the plant cell MTs.

The dynamic changes in MT distribution are shown in Fig. 1, which records the progression of a single living cell over a 97-min interval from prophase through the completion of the cell plate. This sequence began at a time when both the preprophase band and the forming spindle in the perinuclear zone were evident. The preprophase band occupied its characteristic equatorial position, while the developing mitotic apparatus was most concentrated in the presumptive spindle pole regions. In some instances during prophase we observed a tongue of tubulin extending into the nuclear region (Fig. 1 *a–c*), which we infer is due to the infolding of the nuclear envelope brought about by a growing bundle of MTs and does not indicate the dissolution of the envelope. Within a few minutes nuclear envelope breakdown occurred as evidenced by the rapid penetration of fluorescent tubulin into the nuclear region (Fig. 1 *d–g*). Eventually the somewhat diffuse fluorescence of the forming spindle became organized into a recognizable metaphase spindle (Fig. 1*h*), in which the kinetochore bundles were clearly delineated as bright fibers attached to the chromosomes.

During anaphase in *Tradescantia* stamen hair cells (Fig. 1 *i–m*), >90% of chromosome motion consists of movement to the poles or anaphase A (25). Thus the chromosome-to-pole distance shortens, a process that can be seen herein as a shortening of the fluorescent kinetochore fibers (compare Fig. 1 *i* and *m*). Also note in this particular example that the metaphase plate is highly skewed relative to the transverse axis of the cell. We frequently observed similar patterns in *Tradescantia* stamen hair cells and other cells as well (26) but hasten to add that during anaphase the spindle structure and separating chromosomes reoriented and came to lie in a plane that would ensure the formation of a transversely oriented cell plate. By late anaphase, when the chromosomes reached the poles, the kinetochore MT fluorescence had virtually disappeared (Fig. 1 *o–q*).

As anaphase progressed, we also observed a brightly fluorescent interzone apparatus (Fig. 1 *o–r*). Initially these fibers were spread rather evenly across the interzone between the separating daughter sets of chromosomes, but as anaphase advanced they appeared to coalesce laterally to form an elongated bundle in the middle of the cell. This bundle then shortened and again began to expand laterally, giving rise to the phragmoplast (Fig. 1 *r–t*). By a process that is well known and clearly confirmed herein, the phragmoplast grew centrifugally toward the edges of the cell (Fig. 1 *t–w*). Fluorescence diminished in the central region of the structure but increased at the edges (Fig. 1 *v–w*). Eventually the phragmoplast reached the side walls at which time its fluorescence disappeared, and the tubulin subunits then became distributed throughout the cytoplasm of the daughter cells (Fig. 1*x*).

A summary of the timing of mitotic events for this cell revealed the following intervals: nuclear envelope breakdown to the onset of anaphase (metaphase transit time) was 44 min; onset of anaphase to the initiation of cell plate was 20 min; and completion of the cell plate was 24 min. Although metaphase transit time was slower than the average for uninjected controls (32.5 min) (27), the times for anaphase and for the initiation and completion of the cell plate were completely normal. Thus, despite the presence of foreign tubulin and repetitive laser irradiations, this cell, to a large extent, behaved like a control.

Of the mitosis-associated MT structures, the preprophase band has been the most difficult to observe. Beyond that shown in Fig. 1 *a–c*, two further examples are shown in Fig. 2 *a* and *b*. Fig. 2*a* is from a cell in early–midprophase and reveals the preprophase band before the formation of the perinuclear spindle. Fig. 2*b* is a reconstruction of 13 successive planes of focus from a late prophase cell and reveals the projection of the band across the surface of the nucleus as well as the polar caps of the forming spindle apparatus.

That the above results are not due to a nonspecific accumulation of the fluorescently labeled brain tubulin is confirmed by two types of controls. In the first, the cells were injected with fluorescently labeled bovine serum albumin (Fl-BSA). As can be seen in Fig. 2 *c–e*, the entire free volume of the cell including the mitotic apparatus was stained. Interestingly though, the region occupied by the mitotic apparatus and, subsequently, the region of the phragmoplast were somewhat more brightly stained than the rest of the cytoplasm. Because membranous organelles were excluded from these regions, we believe that the slightly enhanced fluorescence is due to a relative increase in cytoplasmic volume that is accessible to the Fl-BSA and not to an association between Fl-BSA and the spindle or phragmoplast structure. A second control consisted of treating injected cells with low temperature to depolymerize the spindle MTs (Fig. 2 *f–k*). In Fig. 2*f*, the tubulin-labeled spindle fibers are observed at anaphase. Chilling the cell to 0–4°C for 5 min caused a total destruction of spindle fibers; however, during the 20-sec interval that this cell was being imaged, the brief warming on the microscope stage permitted the fibers to begin reforming (Fig. 2*g*). Continued rewarming allowed further spindle recovery and the resumption of anaphase chromosome motion (Fig. 2 *h* and *i*). Chilling a second time caused dispersal of the fluorescent phragmoplast structure (Fig. 2*j*) from which the MT fibers again reformed upon warming (Fig. 2*k*).

## DISCUSSION

The results show that fluorescently labeled brain tubulin incorporates into the MTs of dividing stamen hair cells of *Tradescantia*. Through the successive stages of mitosis and cytokinesis these subunits are repeatedly reutilized and are observed in several distinct MT structures including the preprophase band, the perinuclear clear zone at prophase, the kinetochore fibers and half spindle from prometaphase to anaphase, the interzone during anaphase, and finally the phragmoplast during cytokinesis. Besides the close congruence in structure between the images shown herein and those obtained through tubulin immunofluorescence microscopy (2, 3, 5, 6, 18–21), a compelling confirmation that the brain tubulin has entered the normal cellular pool and is acting as a faithful reporter molecule is borne out by the observations

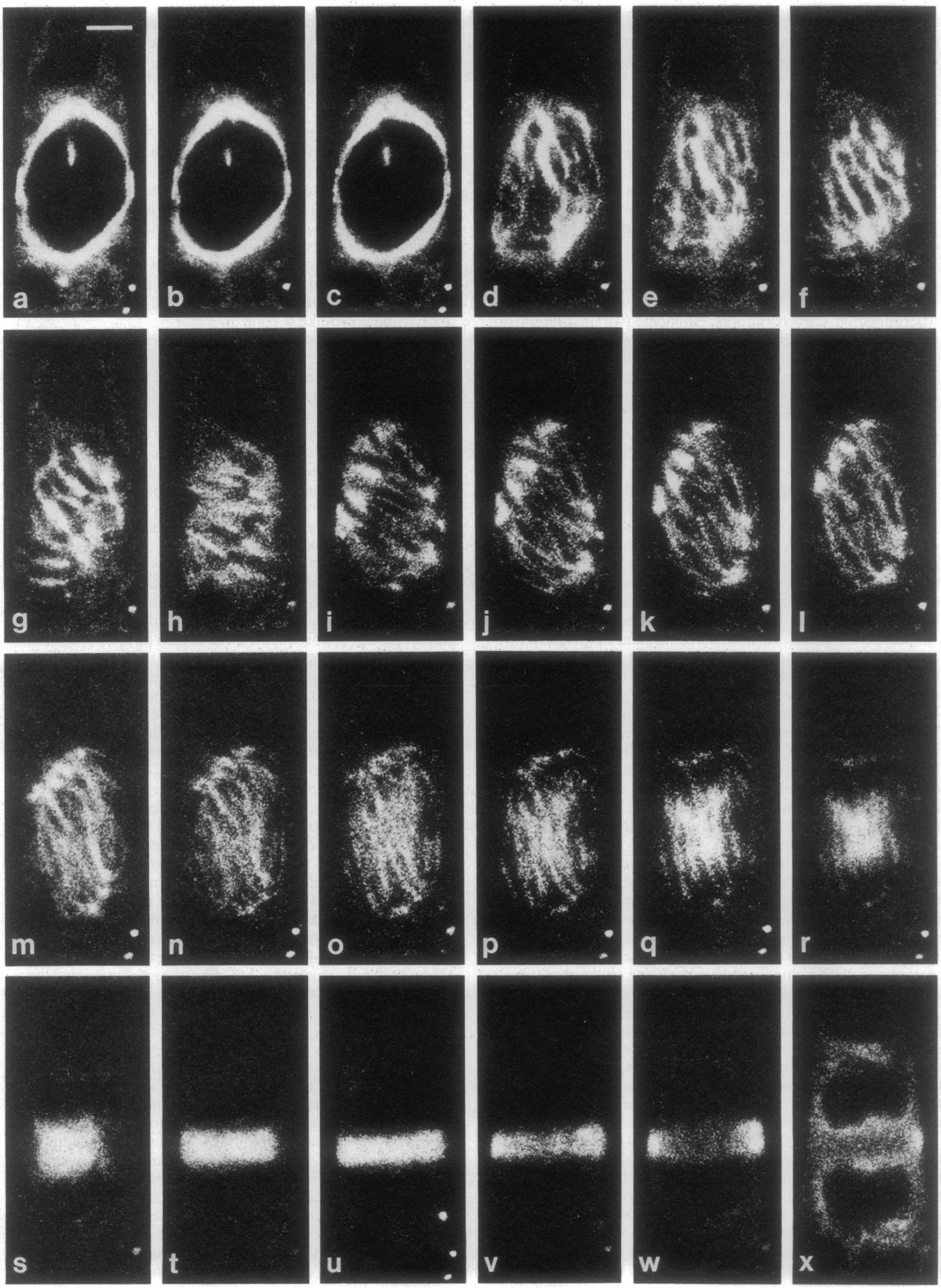


FIG. 1. (*Legend appears at the bottom of the opposite page.*)

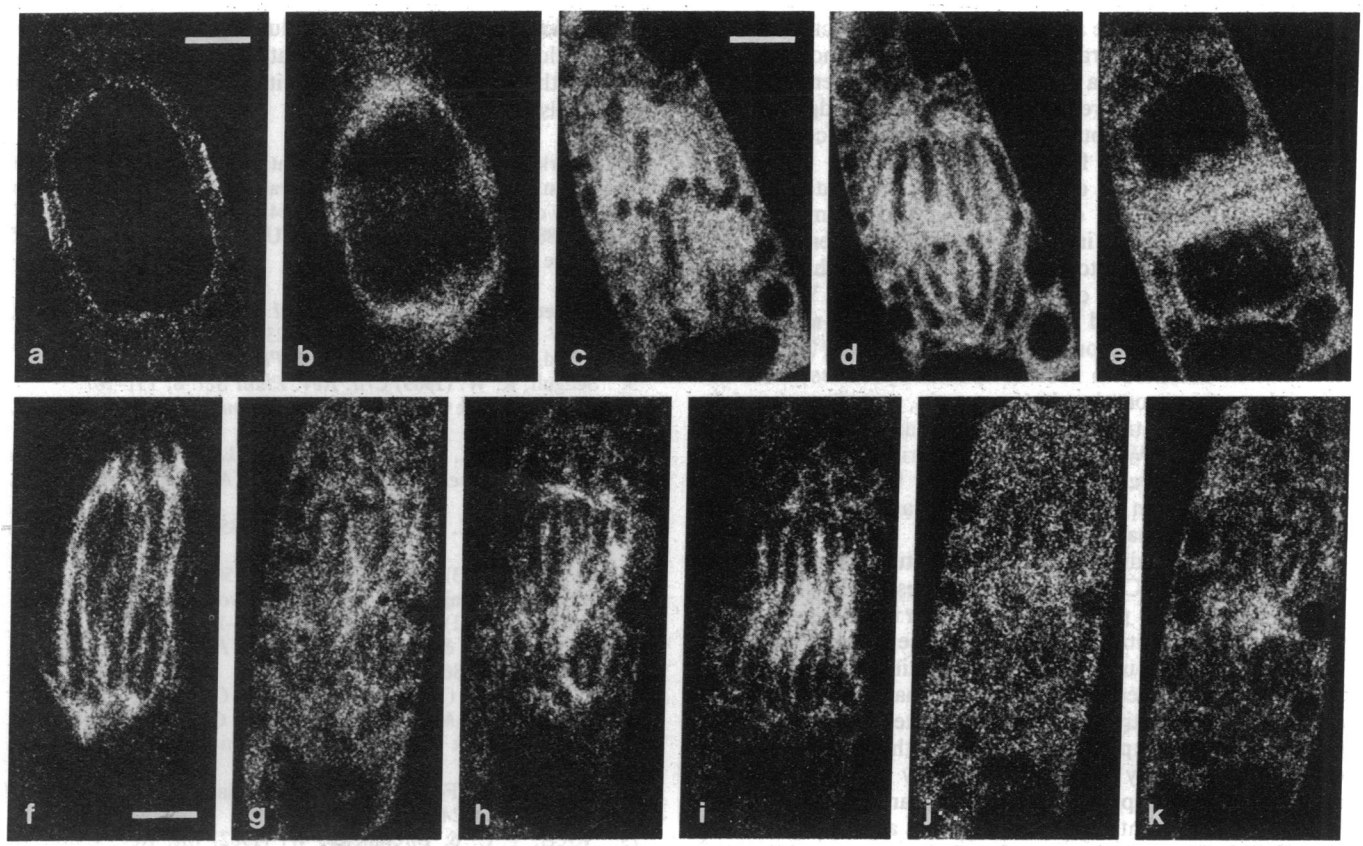


FIG. 2. (*a*) Preprophase band observed during early–midprophase. Here the band stands out clearly against a relatively low background. At this stage there is only a slight indication of the perinuclear spindle apparatus. Although only one figure is shown, this particular cell was followed through nuclear envelope breakdown and spindle formation. (Bar = 10 μm.) (*b*) Preprophase band observed during late prophase. In this example the particular cell was examined successively at 13 separate planes of focus and the images were summed to produce a composite view. The preprophase band thus can be seen at the cell edge in profile and extending across the surface of the nucleus as a faint fluorescent ribbon. The perinuclear apparatus is also evident with the heaviest staining at the region of the presumptive spindle poles. (*c–e*) Control cell injected with fluorescent bovine serum albumin shows fluorescence spread quite evenly throughout the cell. There is, however, a slightly higher level in the region of the mitotic apparatus and phragmoplast that we believe is simply due to the relatively greater volume of cytoplasm accessible to the probe at these locations. (Bar = 10 μm.) Times: *c*, 0:00:00; *d*, 0:23:12; *e*, 0:49:16. (*f–k*) Chilling and rewarming of a tubulin-injected cell provides direct evidence for MT loss and reformation. A cell in mid–late anaphase (*f*) was chilled to 4°C for 5 min and observed (*g*). While the image was being obtained (20-sec interval), the spindle started to reform. As rewarming continued the interzone became more fluorescent (*i* and *j*). Notice also that the chromosomes have progressed to a late anaphase configuration (*i*). A second low-temperature treatment completely reduced the fluorescence of the interzone, resulting in tubulin fluorescence throughout the entire cell (*j*). Upon rewarming the interzone-phragmoplast structure began to reemerge (*k*). (Bar = 10 μm.) Times: *f*, 0:00:00; *g*, 0:06:07; *h*, 0:08:57; *i*, 0:18:07; *j*, 0:24:07; *k*, 0:26:53.

revealing that the fluorescent spindle and phragmoplast structures break down at low temperatures and reform with warming. These studies thus demonstrate the efficacy of using heterologous (animal) derivatized tubulin to examine MT structures and dynamics in living plant cells. In this regard it is important to note that other studies have determined that heterologous tubulins can copolymerize with plant MTs. By following regrowth after oryzalin-induced depolymerization in lysed internode cells of *Nitella*, Wasteneys *et al.* (28) were able to document the incorporation of biotinylated brain tubulin into endoplasmic and nucleus-associated MTs. A *Paramecium* ciliary axonemal tubulin has been shown to incorporate into the spindle and phragmoplast of *Haemanthus* endosperm cells (29). However, in both studies the incorporation was carried out on perfused or lysed cells and the subsequent analysis on fixed tissue.

The ability to observe spindle dynamics in single living cells provides important information concerning the different transitions between the separate MT structures. During prophase, for example, the results herein provide direct evidence for bundles of MTs that extend deep into the nucleus region but are still restrained by an intact nuclear envelope. In later stages of mitosis a particularly interesting MT transition has been that which occurs from anaphase to cytokinesis, in which the fluorescence micrographs reveal a continuum from interzone MT bundles to the emergence of the phragmoplast. These observations thus confirm and strengthen the hypothesis that the phragmoplast is initially

FIG. 1 (*on opposite page*). Cell division in a stamen hair cell of *Tradescantia*. The cell had been injected with carboxyfluorescein-labeled brain tubulin during early prophase and was observed as it progressed through mitosis and cytokinesis by using a CLSM. The fluorescently labeled tubulin incorporated into all the major MT organelles including the preprophase band (*a–c*), the perinuclear spindle apparatus (*a–c*), the forming spindle apparatus (*d–g*), the kinetochore fibers (*h–n*), the interzone fibers (*i–q*), and the phragmoplast (*r–w*). At the end of cytokinesis, the MTs disassembled and the tubulin subunits dispersed throughout the cytoplasm (*x*). In this particular example the metaphase plate was skewed relative to the axis of the cell (*h*). Notice that during anaphase the spindle reoriented (*i–r*), until it was parallel to the cell axis. (Bar = 10 μm.) Times, relative to nuclear envelope breakdown 0:00:00 (hr:min:sec), are given as follows: *a*, −0:08:17; *b*, −0:05:57; *c*, −0:03:30; *d*, 0:03:15; *e*, 0:04:42; *f*, 0:07:35; *g*, 0:11;19; *h*, 0:38:31; *i*, 0:50:26; *j*, 0:51:50; *k*, 0:53:11; *l*, 0:54:48; *m*, 0:56:59; *n*, 0:58:36; *o*, 1:00:03; *p*, 1:01:55; *q*, 1:03:18; *r*, 1:04:45; *s*, 1:06:34; *t*, 1:11:13; *u*, 1:14:04; *v*, 1:18:30; *w*, 1:21:10; *x*, 1:28:59.

directly derived from the anaphase-interzone structure. During the subsequent lateral growth of the phragmoplast the data are consistent with a process of MT depolymerization in the central region with repolymerization at the edges, however, we cannot rule out a process of lateral centrifugal displacement of already formed MTs.

An important aspect of this contribution relates to the technical achievements of introducing and examining reporter macromolecules in living plant cells. Referred to as fluorescent analogue cytochemistry, this approach has been widely used in studies of animal cells (10–13). While the technique has provided important information about MT turnover and participation in chromosome motion (30–32), it need not be confined to MTs or spindle dynamics, since in principle any macromolecule (e.g., actin, myosin, calmodulin, etc.) can be introduced into a cell and its localization directly analyzed. We imagine that a variety of growth and morphogenetic processes in plants can be probed with a degree of precision and fidelity that can only be gained through the examination of living cells.

An unexpected dividend from this study has been the realization that the CLSM can be much less damaging to live cells and cause less photobleaching of an introduced fluorophore than conventional epifluorescence microscopy. We have repeatedly found that cells containing fluorescently labeled tubulin, when examined by normal epifluorescence, are markedly sensitive to irradiation, often resulting in cell death after a few exposures. In addition the carboxyfluorescein is substantially bleached after only a few successive irradiations. Both problems can be dramatically reduced when the fluorescently labeled structures are examined with the CLSM. Through the use of appropriate neutral density filters and the selection of a small illumination aperture, it is possible to create conditions that allow one to repeatedly obtain fluorescent images without destroying the fluorescence and without damaging the cell. The cell shown in Fig. 1, for example, was photographed 24 times over a period of 97 min and completed mitosis in about the normal time interval. Also note that the successive images retain the same apparent degree of fluorescence, indicating that little bleaching of the tubulin has occurred. Even though the laser excitation in the CLSM is intense, its time is short; for 20 scans at the fast rate used, we calculate that a given spot in the cell receives only 0.05 msec of irradiation. The total irradiation needed to produce an image thus can be substantially reduced when compared to that from a conventional epifluorescence microscope.

Despite our success examining MTs at all stages of mitosis, we have not observed the interphase cortical array, although these MTs are shown clearly by electron microscopy (1) and immunofluorescence microscopy (2, 3, 5, 6, 18, 33). We think that the fluorescent signal from the relatively dispersed interphase cortical MTs may be too weak to detect against the background of unpolymerized subunits, which are evenly distributed throughout the cytoplasm. In contrast immunofluorescence staining can reveal the cortical MTs because it benefits from the signal amplification obtained when using fluorescent secondary antibodies.

In conclusion, we show herein that fluorescently labeled brain tubulin has been injected into living dividing plant cells, that it becomes incorporated into MTs, and that it is repeatedly reutilized to form all the MT structures associated with cell division. Observations of the fluorescent signal with the CLSM allows us to follow the location and dynamic transitions of these MTs throughout mitosis and cytokinesis in living cells.

This work has been supported by grants from the National Science Foundation (BBS-87-14235 to the central microscopy facility at the University of Massachusetts, DCB-89-04138 to P.W., DCB-87-02057 and DCB-88-01750 to P.K.H.), and the United States Department of Agriculture (88-37261-3727 to P.K.H.).

1. Hepler, P. K. (1985) in *Botanical Microscopy*, ed. Robards, A. W. (Oxford, New York), pp. 233–262.
2. Lloyd, C. W. (1987) *Annu. Rev. Plant Physiol.* **38,** 119–139.
3. Seagull, R. W. (1989) *Crit. Rev. Plant Sci.* **8,** 131–167.
4. Baskin, T. I. & Cande, W. Z. (1990) *Annu. Rev. Plant Physiol.* **41,** 277–315.
5. Gunning, B. E. S. (1982) in *The Cytoskeleton in Plant Growth and Development*, ed. Lloyd, C. W. (Academic, New York), pp. 229–292.
6. Gunning, B. E. S. & Wick, S. M. (1985) *J. Cell Sci.* Suppl. 2, 157–179.
7. Inoué, S. (1953) *Chromosoma* **5,** 487–500.
8. Inoué, S. & Bajer, A. (1961) *Chromosoma* **12,** 48–63.
9. Inoué, S. (1981) *J. Cell Biol.* **91,** 131s–147s.
10. Taylor, D. L. & Wang, Y.-L. (1978) *Proc. Natl. Acad. Sci. USA* **75,** 857–861.
11. Wang, Y.-L. (1989) in *Methods in Cell Biology, Vol. 29: Fluorescence Microscopy of Living Cells in Culture,* eds. Wang, Y.-L. & Taylor, D. L. (Academic, Boston), Part A, pp. 1–12.
12. Keith, C. H., Feramisco, J. R. & Shelanski, M. (1981) *J. Cell Biol.* **88,** 234–240.
13. Kreis, T. E. & Birchmeier, W. (1982) *Int. Rev. Cytol.* **75,** 209–227.
14. White, J. G., Amos, W. B. & Fordham, M. (1987) *J. Cell Biol.* **105,** 41–48.
15. Hepler, P. K. & Callaham, D. (1987) *J. Cell Biol.* **105,** 2137–2143.
16. Sloboda, R. D., Dentler, W. L. & Rosenbaum, J. L. (1976) *Biochemistry* **15,** 4497–4505.
17. Vigers, G. P. A., Coue, M. & McIntosh, J. R. (1988) *J. Cell Biol.* **107,** 1011–1024.
18. Wick, S. M. (1985) *Cell Biol. Int. Rep.* **9,** 357–371.
19. Simmonds, D. H. (1986) *Planta* **167,** 469–472.
20. Palevitz, B. A. (1988) *Protoplasma* **142,** 74–78.
21. Wang, H., Cutler, A. J. & Fowke, L. C. (1989) *Protoplasma* **150,** 110–116.
22. Hepler, P. K. & Jackson, W. T. (1968) *J. Cell Biol.* **38,** 437–446.
23. Pickett-Heaps, J. D. (1969) *Cytobios* **3,** 257–280.
24. Bajer, A. S. & Mole-Bajer, J. (1986) *J. Cell Biol.* **102,** 263–281.
25. Hepler, P. K. & Palevitz, B. A. (1986) *J. Cell Biol.* **102,** 1995–2005.
26. Palevitz, B. A. & Hepler, P. K. (1974) *Chromosoma* **46,** 297–326.
27. Hepler, P. K. (1985) *J. Cell Biol.* **100,** 1363–1368.
28. Wasteneys, G. O., Jablonsky, P. P. & Williamson, R. E. (1989) *Cell Biol. Int. Rep.* **13,** 513–528.
29. Vantard, M., Levilliers, N., Hill, A.-M., Adoutte, A. & Lambert, A.-M. (1990) *Proc. Natl. Acad. Sci. USA* **87,** 8825–8829.
30. Salmon, E. D., Leslie, R. J., Saxton, W. M., Karow, M. L. & McIntosh, J. R. (1984) *J. Cell Biol.* **99,** 2165–2174.
31. Wadsworth, P. & Salmon, E. D. (1986) *J. Cell Biol.* **102,** 1032–1038.
32. Gorbsky, G. J., Sammak, P. J. & Borisy, G. G. (1987) *J. Cell Biol.* **104,** 9–18.
33. McCurdy, D. W. & Gunning, B. E. S. (1990) *Cell Motil. Cytoskeleton* **15,** 76–87.